Hydrol. Earth Syst. Sci. Discuss., 12, 12703–12746, 2015
www.hydrol-earth-syst-sci-discuss.net/12/12703/2015/
doi:10.5194/hessd-12-12703-2015

Hydrology and Earth System Sciences
Open Access
Discussions

Predicting future US water yield and ecosystem productivity by linking an ecohydrological model to WRF dynamically downscaled climate projections

S. Sun[1,2], G. Sun[3], E. Cohen[3], S. G. McNulty[3], P. Caldwell[4], K. Duan[1], and Y. Zhang[1]

[1]Department of Marine, Earth, and Atmospheric Sciences, North Carolina State University, Raleigh, North Carolina, USA
[2]Key Laboratory of Meteorological Disaster of Ministry of Education, Nanjing University of Information Science and Technology, Nanjing, Jiangsu Province, China
[3]Eastern Forest Environmental Threat Assessment Center, USDA Forest Service, Raleigh, North Carolina, USA
[4]Center for Forest Watershed Research, Coweeta Hydrologic Lab, Southern Research Station, Otto, North Carolina, USA

Received: 18 November 2015 – Accepted: 19 November 2015 – Published: 8 December 2015

Correspondence to: G. Sun (gesun@fs.fed.us)

Published by Copernicus Publications on behalf of the European Geosciences Union.

Abstract

Quantifying the potential impacts of climate change on water yield and ecosystem productivity (i.e., carbon balances) is essential to developing sound watershed restoration plans, and climate change adaptation and mitigation strategies. This study links an ecohydrological model (Water Supply and Stress Index, WaSSI) with WRF (Weather Research and Forecasting Model) dynamically downscaled climate projections of the HadCM3 model under the IPCC SRES A2 emission scenario. We evaluated the future (2031–2060) changes in evapotranspiration (ET), water yield (Q) and gross primary productivity (GPP) from the baseline period of 1979–2007 across the 82 773 watersheds (12 digit Hydrologic Unit Code level) in the conterminous US (CONUS), and evaluated the future annual and monthly changes of hydrology and ecosystem productivity for the 18 Water Resource Regions (WRRs) or 2-digit HUCs. Across the CONUS, the future multi-year means show increases in annual precipitation (P) of 45 mm yr^{-1} (6 %), 1.8 °C increase in temperature (T), 37 mm yr^{-1} (7 %) increase in ET, 9 mm yr^{-1} (3 %) increase in Q, and 106 g C m^{-2} yr^{-1} (9 %) increase in GPP. Response to climate change was highly variable across the 82, 773 watersheds, but in general, the majority would see consistent increases in all variables evaluated. Over half of the 82 773 watersheds, mostly found in the northeast and the southern part of the southwest would have an increase in annual Q (>100 mm yr^{-1} or 20 %). This study provides an integrated method and example for comprehensive assessment of the potential impacts of climate change on watershed water balances and ecosystem productivity at high spatial and temporal resolutions. Results will be useful for policy-makers and land managers in formulating appropriate watershed-specific strategies for sustaining water and carbon sources in the face of climate change.

HESSD

12, 12703–12746, 2015

1 Introduction

The Earth's climate system has been significantly altered over the past 100 years due to human activities, such as emissions of greenhouse gas, aerosol and land use/cover change (LUCC). The Intergovernmental Panel on Climate Change (IPCC, 2014) concluded that global mean surface temperature (T) has increased by 0.78 °C between 1850–1900 and 2003–2012. Additionally, extreme precipitation and droughts have increased (Tebaldi et al., 2006; Trenberth, 2011; Bony et al., 2013; Hegerl et al., 2014). The global climate is projected to continue to change over this century and beyond (IPCC, 2014). Comparing to the period of 1986–2005, the period 2018–2100 is projected to see 0.3 to 4.8 °C increase in global surface temperature (IPCC, 2014). Projections of future changes in precipitation suggest a small increase in the global average, but a substantial shift in where and how intensely precipitation falls (Noake et al., 2012; Scheff and Frierson, 2012; J. Liu et al., 2013).

In response, the hydrological cycle and ecosystems have been and will be markedly changed through various physical, chemical and biological processes (Labat et al., 2004; Milly et al., 2005; Dai et al., 2009; Harding et al., 2011; Sedláček and Knutti, 2014). Mounting evidence has suggested that climate change played an important role in controlling the water cycle by affecting evaporation, transpiration and runoff (McCabe et al., 2002; Hamlet et al., 2007; Syed et al., 2010; Wang and Hejazi, 2011; Chien et al., 2013; Hegerl et al., 2014; Huntington and Billmire, 2014; McCabe and Wolock, 2014; Sun et al., 2014). Climate can also exert a dominant control on vegetation structural and phenological characteristics through variations in air temperature, precipitation, vapor pressure deficit, solar radiation, wind, and CO_2 concentration (Nemani et al., 2003; Harding et al., 2011; Wang et al., 2014). Climate change affects vegetation dormancy onset date, greenness phenology, net primary production (NPP), gross primary production (GPP), and ecosystem respiration (Nemani et al., 2003; Scholze et al., 2006; Pennington and Collins, 2007; Anderson-Teixeira et al., 2011; Gang et al., 2013; Peng et al., 2013; Zhang et al., 2013; Williams et al., 2014; Wu et al., 2014; Piao et al.,

HESSD
12, 12703–12746, 2015

2015; Wang et al., 2015). Future water supply and ecosystem productivity, two key ecosystem services that play an increasing role in adapting to climate change, will be affected by the combined forces from the natural environment (e.g., climate and land surface properties) and socio-economics (e.g., economic development and population increases) (Cox et al., 2000; Somerville and Briscoe, 2001; Sitch et al., 2008; Alkama et al., 2013; Piontek et al., 2014; Schewe et al., 2014; Zhang et al., 2014; Aparício et al., 2015).

In the US, average temperature has dramatically increased since the record keeping began in 1895. The most recent decade was believed to be the nation's warmest on record (see the website: http://www.nasa.gov/home/hqnews/2010/jan/HQ_10-017_Warmest_temps.html). The mean precipitation over the US has increased overall since 1900; some areas have increased with a higher rate than the national average, and some areas have decreased (Groisman et al., 2004; Meehl et al., 2005; Anderson et al., 2015). Over the past century, climate change in the US has caused severe water stress, floods and droughts as well as forest morality (Xu et al., 2013), consequently leading to serious economic losses in some regions. Quantifying the impacts of future climate change on water and ecosystem productivity has become a major research area in hydrology and ecosystem sciences (Lettenmaier et al., 1994; Lins and Slack, 1999; Groisman et al., 2001; McCabe and Wolock, 2011; Sagarika et al., 2014).

Climate change impacts on the water cycle and ecosystem productivity vary from region to region because climate change patterns are not uniform across space or time (Sankarasubramanian et al., 2001; Sankarasubramanian, 2003; Wang and Hejazi, 2011; Xu et al., 2013; Brikowski, 2014), and the spatial variability across regions increases as the spatial resolution increases from large river basins to small catchments. To support future watershed management and to develop sound climate change adaptation strategies over the continental US (CONUS), tools are needed to integrate various climate scenarios from a variety of Atmospheric Ocean General Circulation Models (AOGCMs) and Community Earth System Models (CESMs), and hydrological and vegetation dynamic models (Brown et al., 2013; Blanc et al., 2014; Yu et al., 2014).

HESSD
12, 12703–12746, 2015

Two major research gaps exist in past climate change studies that aim to quantify the interactions among climate, hydrology and ecosystem productivity. First, few studies provided projections of future climate change impacts on water and carbon balances at watershed scale using a consistent approach. Various land surface models (LSMs) simulate and predict water fluxes for a large region, but the scale is often too coarse with a spatial resolution ranging from 0.25 to 2.5°, and the spatial representation of the projections (e.g., grids) are not readily consumable by resource managers who operate at the watershed scale. In addition, key hydrological processes (e.g., lateral surface and sub-surface flows among grid boxes) embedded in LSMs have not been considered, potentially resulting in uncertainties in water balance projections (Overgaard et al., 2006; Li et al., 2011). Second, future climate projections have high uncertainty. To save computational resources and enhance the computational efficiency, statistical (or empirical) downscaling methods have been used to generate climate forcing to land surface models or watershed ecosystem models. This type of methods does not consider the effects of atmospheric dynamical processes (Xue et al., 2014) and could introduce uncertainties into the crucial land surface variables.

The objective of this study is to address these gaps in our understanding of watershed scale responses to climate change by exploring the potential benefits of linking dynamically downscaled climate projections with a common ecosystem model for climate change assessment at a fine spatial scale (82 773 12-digit HUC watersheds of the CONUS). The specific objectives of this study are to (1) examine future climate changes in precipitation, and temperature during 1979–2007 and 2031–2060 for one plausible emission scenario over the CONUS using WRF (Weather Research and Forecasting) dynamically downscaled climate projections, (2) predict future changes of the CONUS water yield (Q), ET, and GPP by linking the WRF dynamically downscaled climate change scenarios and the WaSSI model. The goal is to generate information that can be useful for resource managers and policy makers to plan for potential shifts in water resources and ecosystem productivity at scales that are relevant from the watershed to national level.

HESSD
12, 12703–12746, 2015

2 Data and methodology

2.1 Study area

The research area includes 82 773 12-digit HUC watersheds within the 18 Water Resources Regions (WRRs) over the CONUS (WBD; Watershed Boundary Dataset, 2010) (Fig. 1a). The 12-digit HUC watershed is defined in a national standard, six-level hierarchical system of hydrologic units in the US, ranging from 18 WRRs in the conterminous US at the first level to approximately 83 000 sub-watersheds, or 12-digit HUC watersheds, at the sixth level (Seaber et al., 1987). Hydrologic Units in each level are nested within the next higher level, and are assigned a unique code consisting of two to 12 digits for WRR and 12-digit HUC watersheds, respectively. The WRRs vary in size with the maximum of 1.3×10^6 km^2 (WRR10) and the minimum of 1.1×10^5 km^2 (WRR6), while the 12-digit HUCs are 95 km^2 on average. Land surface characteristics (Fig. 1b) vary dramatically among these WRRs (Fry et al., 2011). The WRRs in the east had the larger percentages (around 10 %) of urban use with WRR2 (13 %) and WRR4 (11 %) ranked as the top two. The wetlands are mainly located in the WRRs in the eastern US, while the western regions had the higher percentages of shrubland (> 30 %). The WRRs in the east had higher forest (including mix, evergreen and deciduous forests) percentages (> 33 %) than the west (< 33 %). The deciduous and the evergreen forests were mainly found in the east and the west, respectively. Most of the crop lands were located in the east and central CONUS (Fig. 1b).

2.2 Dynamically downscaled climate by WRF

The IPCC Special Report on Emissions Scenarios (SRES) scenarios were designed to project future global environment with a special reference to the production of greenhouse gases and aerosol precursor emissions (Nakicenvoic et al., 2000). The SRES scenarios include four narrative storylines (i.e., A1, A2, B1 and B2) describing the relationships between the forces affecting greenhouse gas and aerosol emissions and their

HESSD
12, 12703–12746, 2015

evolution in the 21st century. Each storyline represents a specific and typical demographic, economic, technological, social and environment progresses with divergence in increasingly irreversible ways. The A2 SRES scenario was selected because it represents a potentially worst-case scenario, and because post-2000 global carbon emissions estimates indicate that current emissions are tracking the higher of the SRES emissions projections (Raupach et al., 2007) making the A2 scenario potentially more likely given current trends.

The Global Circulation Models (GCMs) have significant issues in representing local climates due to their coarse spatial resolution (Leung and Qian, 2003). Two types of downscaling method are available: dynamical and statistical (or empirical) downscaling (Huang et al., 2011) to downscale the GCMs climate data to a higher spatial resolution for regional and local applications. Dynamical downscaling was used here for generating the current and the future climate due to better representation of finer scale physical processes in climate variables (Gao et al., 2011).

Among the many GCMs available in the World Climate Research Programme's (WCRP) Coupled Model Intercomparison Project phase 3 (CMIP3) Climate Projections (Meehl et al., 2007), the HadCM3 model has been regarded as having the most realistic description of the ENSO mechanisms in the current climate, and reasonably capture ENSO-associated precipitation anomalies over the North America (van Oldenborgh et al., 2005; Joseph and Nigam, 2006; Dominguez et al., 2009). Based on the importance of precipitation in hydrology and ecosystem productivity assessment, we chose the HadCM3 model to provide forcing fields for running the Advanced Research version (ARW) of the Weather Research and Forecasting (WRF) regional climate model (Skamarock et al., 2005).

The WRF model was run for the years 1969 to 2079 at a 35 km resolution. Six-hour HadCM3 input were used, and the dynamically downscaled output by the WRF model was also stored at 6 h time interval across CONUS and northern Mexico (Wi et al., 2012). The physical parameterizations of the model included: WRF Single-Moment three-class microphysics (Hong et al., 2004), Kain-Fritsch cumulus parameterization

HESSD
12, 12703–12746, 2015

(Kain and Fritsch, 1993), Goddard Shortwave radiation (Chou and Suarez, 1994), Rapid Radiative Transfer Model (RRTM), Longwave (Mlawer et al., 1997), Eta surface layer (Janjic, 2002), Mellor-Yamada-Janjic (MYJ) planetary boundary layer (Janjic, 2002), and the Noah land surface model Version 1.0 (Chen and Dudhia, 2001). To ensure the maintenance of synoptic-scale circulation features (e.g., ridges and troughs) in the RCM, we performed spectral nudging on the zonal and meridional winds, the temperatures and the geo-potential height fields for all pressure levels below 0.36 of the surface pressure (for a surface pressure of 1000 mb it would be all pressures below 360 mb) effectively nudging only at very high elevations above the surface.

2.3 Climate data bias corrections

Although the WRF projections were found to be adequate for a hydrological study (1981–2005) in the Colorado River Basin (Wi et al., 2012), we found some large regional biases that required bias correction prior to coupling with the ecosystem model. We used the monthly Bias Correction Spatial Disaggregation (BCSD; Wood et al. (2002, 2004) approach that has been applied for hydrologic forecasting in the eastern US (Wood et al., 2002). Steps in the BCSD procedure includes (1) scale up historical Precipitation Elevation Regression on Independent Slopes Model (PRISM) monthly precipitation (P) and temperature with 4 km × 4 km resolution (Daly et al., 1994; PRISM Climate Group, 2013) to match the simulated WRF data (35 km × 35 km) for the time period of 1978–2007, (2) construct cumulative distribution functions (CDFs) for climate variables in each grid cell, month for both historic WRF and upscaled PRISM datasets, (3) the paired CDFs combined to form a "quantile map", where at each rank probability or percentile, the bias between the WRF and the PRISM (at that location, for that variable, and during that month) was calculated, (4) The computed bias in each month, grid cell and variable were applied to the WRF future outputs (2031–2060). The detailed procedures can be found in (Brekke et al., 2013; http://gdo-dcp.ucllnl.org/downscaled_cmip_projections). Both the corrected WRF monthly precipitation and temperature in historic and future periods were scaled to the 12-digit

HUC watershed scale because the WaSSI model operated on the 12-digit HUC watershed level.

2.4 The WaSSI model

The Water Supply Stress Index (WaSSI) model is an integrated, water-centric process-based ecohydrological model designed for modeling water and carbon balance and water supply stress at a high resolution across a broad scale (Sun et al., 2011a, 2015a, b; Caldwell et al., 2012). It operates on a monthly time step at the 8-digit HUC or 12-digit HUC watershed scale for the CONUS. The WaSSI model simulates the full monthly water (ET, Q and soil moisture storage) and carbon balances (GPP, ecosystem respiration and net ecosystem productivity) for each land cover class at the given watershed scale. This model has been tested in a variety of geographical regions, and has been widely used for quantitatively assessing combined or individual effects of climate change, land use/cover change (LUCC), and population dynamics on water supply stress and ecosystem productivity (i.e., carbon dynamics) over the CONUS (Sun et al., 2008, 2011a, 2015a, b; Lockaby et al., 2011; Caldwell et al., 2012; Averyt et al., 2013; Tavernia et al., 2013; Marion et al., 2014), Mexico, China (N. Liu et al., 2013) and Africa (McNulty et al., 2015).

The key algorithms of the WaSSI model were derived from accumulated knowledge of ecosystem carbon and water cycles gained through the global eddy covariance flux monitoring networks and watershed-based ecohydrological studies across the US The ecosystem ET sub-module, the core of the WaSSI model, is described as a function of potential ET (PET), LAI, precipitation, and soil water availability by land cover type (Sun et al., 2011a). The snow model embedded with WaSSI (McCabe and Wolock, 1999; McCabe and Markstrom, 2007) estimates snow melt rates and mean monthly snow water equivalent (SWE) mean watershed elevation and monthly air temperature. Infiltration, surface runoff, soil moisture and baseflow processes for each watershed are simulated by the Sacramento Soil Moisture Accounting Model (SAC-SMA; Burnash, 1995). The ecosystem productivity module computes carbon dynamics (GPP and res-

HESSD
12, 12703–12746, 2015

piration) using linear relationships between ET and GPP derived from global eddy covariance flux measurements (Sun et al., 2011a, b). The User Guide of WaSSI Ecosystem Services Model-Version 2.1 (http://www.forestthreats.org/research/tools/WaSSI) provides detailed description of model algorithms and data requirements (Caldwell et al., 2012).

The necessary inputs to run the WaSSI model include monthly precipitation, monthly mean air temperature, monthly mean leaf area index (LAI) by land cover, land cover composition within each watershed, and 11 SAC-SMA soil parameters. The historical (1979–1997) and the future (2031–2060) climate data dynamically downscaled by WRF model, were bias corrected, and thus were scaled to the 12-digit HUC level. The 2006 National Land Cover Dataset (NLCD; http://www.mrlc.gov/nlcd06_data.php) with 17 land cover classes were aggregated into 10 classes (Fry et al., 2011): crop, deciduous forest, evergreen forest, mixed forest, grassland, shrubland, wetland, water, urban and barren. WaSSI The monthly LAI time series data required by WaSSI for each land cover type were derived from the Moderate Resolution Imaging Spectroradiometer (MODIS) – MOD15A2 FPAR/LAI 8 day product (Myneni et al., 2002). The 1 km × 1 km SAC-SMA soil dataset provided by the State Soil Geographic Data Base (STATSGO) – based on the Sacramento Soil Moisture Accounting Model Soil Parameters was aggregated to the 12-digit HUC watershed. No WaSSI model parameters were calibrated during the model evaluation process.

The WaSSI has been evaluated at multiple scales using gaging station data for streamflow and remote sensing products for evapotranspiration across the US (Sun et al., 2011a, 2015a; Caldwell et al., 2012). At the 12-digit HUC scale, the model was validated using monthly and annual water yield data collected at 72 selected USGS watersheds, and ET and GPP data for 170 National Forests over the CONUS (Sun et al., 2015a). Overall, the validation results suggested that this model could capture characteristics of water and carbon balances at the selected spatial levels under various climatic conditions (Sun et al., 2015a, b).

2.5 Impact analysis

We first examined modeled changes in monthly ET and GPP at the 12-digit HUC watershed scale using the WRF dynamically downscaled, bias corrected historical and future climate data, respectively. We next computed future annual changes at three spatial levels: the entire CONUS as whole, the 12-digit HUC watershed, and the individual WRR. The multi-year means of annual precipitation, temperature, ET, *Q*, and GPP averaged across the whole CONUS, WRR, or each 12-digit HUC watershed for the 1979–2007 time period were compared to those for the 2031–2060 period. The absolute or percent (except for temperature) changes for each variable were calculated. The absolute differences were expressed as the future means minus those in the historical period, while the percent differences were calculated using the absolute difference divided by baseline mean in the 1979–2007. The future monthly changes of these ecosystem flux variables were also assessed for the whole CONUS and each WRR.

3 Results

3.1 Baseline characteristics of hydro-climatology and ecosystem productivity (1979–2007)

For the baseline period, multi-year means of annual precipitation (Fig. 2a), ET (Fig. 3a), *Q* (Fig. 3e) and GPP (Fig. 4a) all generally showed longitudinal decreases from east to west across the CONUS. The coastal areas in the Pacific Northwest region has the highest precipitation (> 1800 mm yr^{-1}), followed by the larger values for precipitation (> 1200 mm yr^{-1} in Fig. 2a) in the southeast. For ET, the highest value (> 750 mm yr^{-1} in Fig. 3a) was mainly located in the southeast. *Q* with (> 600 mm yr^{-1} in Fig. 3e) were in the Pacific Northwest region, and the Rocky and the Appalachian Mountains, with the highest values (> 1000 mm yr^{-1}) in 12-digit HUC watersheds along the Pacific coast.

HESSD
12, 12703–12746, 2015

The 12-digit HUC watersheds with higher values (> 1000 g C m^{-2} yr^{-1}) of GPP (Fig. 4a) were mainly located in the areas of the southeast and the Pacific Northwest. By contrast, the average annual temperature climatology of the CONUS presented a clear latitudinal increase ranging from −0.8 °C in the north to 22 °C in the south. Temperature in the Rocky Mountains was lower than 4 °C relative to the surrounding regions due to topographical effects.

The area weighted average precipitation, temperature, ET, Q and GPP across CONUS in the period of 1979–2007 was 801 mm yr^{-1}, 11.2 °C, 515, 290 mm yr^{-1} and 1232 g C m^{-2} yr^{-1}, respectively (Table 1). Comparing the area-average precipitation among the 18 WRRs, the WRR3, 6 and 8 had the highest precipitation (> 1200 mm yr^{-1}), while the WRR13-16 had the lowest (< 400 mm yr^{-1}). In the WRR3, 8, and 12, the area average temperatures were the highest (> 17 °C), while WRR9 had the lowest temperature (4.2 °C). The WRR3, 6 and 8 had the highest ET (> 750 mm yr^{-1}), with the lowest values found in WRR16 (< 300 mm yr^{-1}). The WRR1 had the largest Q of 636 mm yr^{-1}, while the smallest Q was found in the WRR13-16 (< 100 mm yr^{-1}). Similar to the average ET, the highest GPP (> 2100 g C m^{-2} yr^{-1}) were also found in the WRR3, 6 and 8, but the western WRRs (e.g., WRR13-16 and 18) exhibited lowest values (< 800 g C m^{-2} yr^{-1}).

The baseline CONUS-wide intra-annual precipitation presented a complicated pattern (Fig. 5). Except in February, precipitation in all the months was more than 65 mm yr^{-1}, and peaked in May with (78 mm yr^{-1}). Overall, temperature (Fig. 5b), ET (Fig. 5c), and GPP (Fig. 5e) all increased gradually starting from January, peaked (24.8 °C, 80 mm yr^{-1} and 205 g C m^{-2} yr^{-1}, respectively) in July and then decreased sharply. Fluctuations of Q clearly differed from other variables (Fig. 5d) responding to temporal patterns in P, SWE (in snow-dominated watersheds), and ET such that Q increased in January, peaked in April (36 mm yr^{-1}), decreased to the lowest (15 mm yr^{-1}) in August, and then increased. The intra-annual distribution was different (e.g., phases and magnitudes) among the 18 WRRs, due to the complex differences in topography and climate among them (not shown). For WRR16-18, most precipitation fell in

January–April and October–December, while precipitation in other WRRs mainly concentrated in May–September. In all the WRRs, the intra-annual temperature followed a unimodal curve, with peaks in July or August and the lowest values in January or December. For ET and GPP, the higher values were mainly found from May to November, except for the WRR18. Comparing the monthly ET or GPP distributions among the 18 WRRs, they could be divided into three categories: unimodal, sine and trough curves.

3.2 Future climate change

Projected future precipitation and temperature followed a similar pattern as the baseline (Fig. 2). Precipitation showed a longitudinal decrease from the east to the west, but temperature presented a clear latitudinal decrease. However, for each 12-digit HUC watershed, these two climate variables would increase or decrease by different magnitudes in the future (Fig. 2c and d for precipitation, and Fig. 2g). Annual precipitation is predicted to increase in 82 % of the 82 773 12-digit HUC watersheds, those watersheds that were predicted to have a decrease in precipitation were mainly located in the southeast and the west coastal regions. The northeast and the northwest coastal regions were predicted to have a greater absolute increase (> 150 mm yr^{-1}) or decrease (> 200 mm yr^{-1}) in precipitation, respectively (Fig. 2c). The greater percent increases in precipitation (> 18 %) were found in some watersheds in the southwest and the northeast regions (Fig. 2d). Future temperature was predicted to increase consistently across watersheds, ranging from 1.0 ^{o}C to 3.0 °C. The northwest and the north-central regions were predicted to have temperature increase more than 2.1 °C (Fig. 2g).

For the CONUS as a whole, the area weighted mean annual precipitation and temperature for 2013–2060 was 844 mm yr^{-1} and 13.1 °C, respectively (Table 1). The mean annual P for the entire CONUS was predicted to increase by 45 mm yr^{-1} (6 %) and T increase by 1.8 °C (Table 2). All WRRs exhibited increases in P with the exception of WRR17 with a slight decrease in P (13 mm yr^{-1} or 1 %). The large absolute change in precipitation (> 60 mm yr^{-1}) was in WRR2, 4, 5 and 7, while the WRR8 and 14 had lower predicted increases (< 15 mm yr^{-1}). The higher relative increases in pre-

HESSD
12, 12703–12746, 2015

cipitation ($\geq 10\,\%$) existed in the WRR2, 5, 15 and 16, however, WRR1 and 8 had lower predicted increases ($\leq 1\,\%$). For the future temperatures, all the 18 WRRs were predicted to increase in temperature relative to the baseline period, especially in the WRR9, 10, 14 and 16 ($\geq 2\,^{\circ}$C).

Both future P and T had similar intra-annual fluctuations to those of the baseline period (top panels in Fig. 5a and b). However, the magnitudes of differences in both P and T differed in different seasons were different (the bottom of Fig. 5a and b). In most months, precipitation was predicted to increase from 3 to 11 mm yr^{-1}, especially in January, May and September (> 7 mm yr^{-1}). For February, March, October and November, P was predicted to decrease from -5 to -1 mm yr^{-1}. The temperatures for each month were predicted to increase by at least 1.5 °C, particularly for January and June–October ($> 2.0\,^{\circ}$C) (Fig. 5b).

The comparisons of seasonal climatic change patterns among the 18 WRRs suggested the timings of change were similar among WRRs (not shown), but the magnitudes of changes varied greatly. The future monthly precipitation was predicted to increase in January and May–October in more than 10 WRRs. The increases were most pronounced in January, July and September (Fig. 6a). In other months, however, the future monthly precipitation would decrease in most of the WRRs. The future monthly temperature for all the WRRs was predicted to increase from 0.5 to 3.0 °C. January and June–October temperatures in most WRRs were predicted to increase more than 1.5 °C for most WRRs.

3.3 Future (2031–2060) changes in ET and Q

3.3.1 Annual change

The spatial patterns in ET and Q for the baseline were similar to those in the future (Fig. 3). However, the changes of annual ET (Fig. 3c and d) and Q (Fig. 3g and h) for each 12-digit HUC watershed varied spatially. Annual ET was predicted to increase in the majority (98 %) of the 82 773 12-digit HUC watersheds, and the watersheds with

HESSD
12, 12703–12746, 2015

reductions in annual ET were mainly concentrated in the northwest coastal region. Annual ET was predicted increase more (> 32 mm yr^{-1}) in the northeast region (Fig. 3c and d), especially in the southeast coastal region and the southern extent of the northeast region (> 48 mm yr^{-1}). Relative changes (%) in ET were highest (> 6 %) in most of the western regions (excluding the west coast) and the northeast, and the highest increases (> 12 %) were predicted in the southernmost portion of the southwest region.

Annual *Q* was predicted to increase in 52 % of the 82 773 12-digit HUC watersheds by 2031–2060 (Fig. 3g and h). In general, annual *Q* in the northeast and the southernmost portion of the southeastern region was predicted increase, while other regions were predicted to decrease (Fig. 3g and h). The largest increases (> 100 mm yr^{-1}) and the decreases (> 100 mm yr^{-1}) in *Q* were mainly found in the northeast and the west coastal and the southeast regions, respectively. *Q* in the southernmost portion of the southwest region was predicted to increase more than 20 %, while the central part of the west CONUS would generally decrease more than 20 %.

Projected future multi-year mean annual ET and *Q* across CONUS were 551 and 297 mm yr^{-1}, respectively (Table 1), representing an increase in ET by 37 mm yr^{-1} or 7 %, and in *Q* by 9 mm yr^{-1} or 3 % (Table 2). All WRRs were predicted to have an increase in ET. The WRR2, 5 and 7 were predicted to have the largest absolute increases in ET (> 45 mm yr^{-1}), while the WRR17 (18 mm yr^{-1}) was predicted to have the lowest increases. The highest predicted relative increases in ET (≥ 10 %) were in WRR5, 9, 16 and 17, however, WRR17 was predicted to have the lowest increases (4 %). Annual *Q* was predicted to increase in nine WRRs, decrease in eight WRRs, and remain unchanged in one WRR relative to the baseline period (Table 2). Among the 18 WRRs, WRR2 and WRR5 were predicted to have the largest absolute increase (> 60 mm yr^{-1}), and WRR8 and WRR17 had the largest decline (> 20 mm yr^{-1}). The greatest relative increases (> 10 %) and decreases (> 10 %) in annual *Q* were predicted in WRR2, 5 and 15, and WRR14, respectively.

3.3.2 Seasonal change

The variations of future CONUS-wide multi-year mean monthly ET and Q were presented in Fig. 5c and d. The predicted future monthly ET increased the most (> 2 mm yr^{-1}) in January. The April–October ET was predicted to increase more than other four months. Monthly Q was predicted to increase in most months (9 months), especially in January and September (increase > 3 mm yr^{-1}).

We also found that the seasonal patterns of ET and Q for the baseline and the future periods were similar (not shown here), but a magnitudes have changed. Figure 6c and d presents the number of the WRR within a given change interval for ET and Q by month, respectively. Generally, the future monthly ET was predicted to increase by different rates for each month at each WRR (Fig. 6c). Moreover, ET from May to September (roughly the growing season) was predicted to increase more (> 2.4 mm yr^{-1}) than other months in most of the 18 WRRs. Q was predicted to increase in January, February, July, September and December in most of WRRs, but was predicted to decrease in April and November.

3.4 Future changes in GPP

3.4.1 Annual change

The overall spatial distribution of GPP did not change in the future (Fig. 4b) when compared to the baseline (Fig. 4a). However, the magnitudes of GPP changes in the future varied spatially (Fig. 4c and d). Annual GPP was predicted to increase in the majority (98 %) of the 82 773 12-digit HUC watersheds. The few watersheds that were predicted to experience reductions in annual GPP were mainly located in the northwest coastal region. A relatively high increase (> 120 g C m^{-2} yr^{-1}) in GPP was predicted in the northeast, especially in the southern part of the region (> 180 g C m^{-2} yr^{-1}; Fig. 4c). In contrast to the absolute difference, most of the west CONUS (excluding the coastal regions) were predicted to have the largest relative increase (> 12 %) in annual GPP.

The highest changes (> 20 %) were mainly located in southern portion of the southwest region.

Over the CONUS, multi-year mean annual GPP was predicted to be 1339 g C m^{-2} yr^{-1} in the future (Table 1), representing an increase of 106 g C m^{-2} yr^{-1} or 9 % (Table 2). Future annual GPP in every WRR was predicted to increase from 49 g C m^{-2} yr^{-1} to 202 g C m^{-2} yr^{-1} or from 5 to 12 % (Table 2). The WRR2-WRR10 were predicted to have the larger absolute increases in GPP (> 100 g C m^{-2} yr^{-1}), especially for WRR5 with the maximum of 202 g C m^{-2} yr^{-1}, while the WRR13 (49 g C m^{-2} yr^{-1}) had the lowest increases. Relative increases in GPP ranged from 5 to 17 % among all the WRRs. The higher GPP increases (> 10 %) occurred in WRR4, 5, 7, 9, 10 and WRR14-16, with the largest of 17 % in WRR16, while other WRRs had the lower increments than 10 %, particularly in WRR3 and 8 with the minimum of 5 %.

3.4.2 Seasonal change

Figure 5e (the top of each panel) showed the future multi-year mean monthly GPP averaged over the whole CONUS. Despite the similar intra-annual fluctuations of multi-year mean monthly GPP during the baseline and the future periods, the future magnitude in each month was predicted to change to some degree (the bottom of Fig. 5e). Overall, the future monthly ET was projected to have the larger increments (> 9 g C m^{-2} yr^{-1}) in January and May–October relative to other months. The future intra-annual fluctuation patterns of GPP for each WRR were similar to the baseline periods (not shown here). As indicated by the number of the WRR within a given GPP difference interval (Fig. 6e), the future monthly GPP generally would increase by different rates for each WRR. Moreover, GPP from May to September would have greater increments (> 4 g C m^{-2} yr^{-1}) in most of the 18 WRRs.

HESSD
12, 12703–12746, 2015

4 Discussions

4.1 Uncertainties

In the present study, we assumed that the water balance and ecosystem productivity at each 12-digit HUC watersheds were unaffected by human activities as represented by a fixed land cover (year 2006), and changes in ecosystem fluxes were fully attributed to climate change alone. However, most catchments in the US will experience some levels of human influences (National Research Council, 2002). Hydrology and ecosystems can be influenced significantly by human activities on various temporal and spatial scales (Foley et al., 2005; Harding et al., 2011). Hydraulic projects such as dam constructions, reservoir management (Hu et al., 2008), groundwater withdrawals for irrigation and domestic use, and land use/cover change all affect watershed balances (Foley et al., 2005; Piao et al., 2007; Wang and Hejazi, 2011; Schilling et al., 2008) and ecosystem productivity (Zhang et al., 2014).

Similarly, natural disturbances (e.g., wildfire, climate extremes, and pest and pathogen outbreak) could also impact water balance and ecosystem productivity in the past and the future. For example, the direct effects of wildfire include plant mortality and thus exert adverse impacts on vegetation productivity, consequently leading to a decrease in carbon uptake and stocks (Lenihan et al., 2008; Dore et al., 2010; Lee et al., 2015). Wildfires alter the watershed hydrologic processes by reducing vegetation canopy interception, transpiration, and infiltration rates (Yao, 2003; Neary et al., 2005; Bond-Lamberty et al., 2009; Brookhouse et al., 2013; Nolan et al., 2014, 2015). As an important natural disturbance, droughts generally increase vapor pressure gradient between leaves and atmosphere and thus cause stress on plant hydraulic systems (Anderegg et al., 2012; Reichstein et al., 2013). As a result, high tension in the xylem can trigger embolism and partial failure of hydraulic transport in the stem, and may result in vegetation mortality, which can aversely impact water yield and carbon sequestration (Cook et al., 2007; Allen et al., 2010; Guardiola-Claramonte et al., 2011; Adams et al., 2012). In addition, droughts often lead to pest and pathogen outbreaks (Over-

HESSD
12, 12703–12746, 2015

peck et al., 1990; Hason and Weltzin, 2000; Marengo et al., 2008; DeRose and Long, 2012; Jactel et al., 2012), and thus predispose an individual plant species to disease or mortality (Schoeneweiss, 1981; Ayers and Lombarder, 2000). Although our modeling approach considered water stress on productivity, tree mortality was not considered and the impacts of droughts on *Q* and GPP might be underestimated.

Elevated CO_2 can also affect water yield and ecosystem productivity by changing water use efficiency and vegetation processes (e.g., stomatal conductance and LAI; Sun et al., 2014). However, we did not consider the CO_2 fertilization effects, potentially resulting in errors in estimating ET, GPP or water yield (Cox et al., 2000; Gedney et al., 2006; Oki et al., 2006; Betts et al., 2007; Piao et al., 2007). Neglecting human activities and natural disturbances and their combined effects may introduce uncertainties into our results. However, the potential errors are largely dependent on specific trajectories of climate change and land cover change (Qi et al., 2009; Thompson et al., 2011; Alkama et al., 2013). The complex interactions of climate, disturbance, ecohydrological processes require a more mechanistic integrated modeling approach that is beyond the scope of this study.

4.2 Management implications

Numerous modeling studies around the world have showed that climate change could increase or decrease water availability to some ecosystems and human populations under different climate scenarios (Arnell, 1999; Blanc et al., 2014; Ingjerd et al., 2014; Kundzewicz and Gerten, 2015). Our analyses showed that, over the whole CONUS, *P* would increase by 45 mm (6 %) leading to a small increases in *Q* by 9 mm yr^{-1} (3 %). However, there are large regional differences in *Q* responses to future climate change among the 18 WRRs. The range in the magnitude of response is large, ranging from a decrease of −32 mm yr^{-1} to an increase of 113 mm yr^{-1} or from −12 to 21 %. Despite the increase in annual P, annual *Q* in WRR1, 3, 8, 11, 14, 16 and 18 was predicted to decrease by various degrees, due to the increased ET. Consequentially, under the climate scenario studied water supply stress will likely increase in these WRRs. In addition, monthly Q responses to future climate also vary among watersheds. Water yield in about half of the 18 WRRs (mainly located in the west CONUS) was predicted to decrease and increase in WRR2-8. The increased Q in the wet months could increase flooding risk, while decreased Q in dry months could aggravate water shortage conditions. For example, the monthly Q in California (mostly in the WRR18) was predicted to decrease by around 5 mm during spring through early summer (the major runoff generation season) due to coupling of changes in P and ET and/or precipitation forms in the mountainous regions in Sierra Nevada mountains. The decrease in flow may cause severe water shortage similar to what is happening in 2014–2015 in California (Aghakouchak et al., 2014; Mao et al., 2015). Hydrological changes could bring many impacts on water-related economic sectors. For example, droughts would reduce low flows and degrade water quality (high water temperature and nutrient concentrations), and thus have negative effects on fisheries (Magoulick et al., 2003; Dolbeth et al., 2008; Gillson et al., 2009), navigation (Theiling et al., 1996; Roberts, 2001), and recreation (Thomas et al., 2013).

The modeling results suggested that GPP over the whole CONUS would increase 106 g C m^{-2} yr^{-1} (9 %) in the future. The increase by WRR ranged from 49 g C m^{-2} yr^{-1} to 202 g C m^{-2} yr^{-1} or from 5 to 17 % among the 18 WRRs. These findings suggested that carbon stock and vegetation capacity to sequester atmospheric CO_2 for the entire CONUS and each WRR could be enhanced under the SRES A2 climate scenario. Most WRRs were predicted to have GPP increases during late spring to summer, which implied that the capability of ecosystems to sequester carbon in these months will be significantly enhanced in future. By contrast, GPP was predicted to decrease in several WRRs for several months. For example, during August and September, predicted GPP in WRR17 decreased. The ecosystem sequestration carbon capability would be reduced in these months under the SRES A2 climate scenario. For forests, variations of GPP caused by climate change will be ultimately reflected in timber production, soil carbon storage, and other ecosystem processes such as dissolved carbon loading in aquatic ecosystems. According to this study, the forest biomass and timber production

HESSD
12, 12703–12746, 2015

could increase, thus climate change may have implications on timber prices in timberland dominated regions (Sohngen and Mendelsohn, 1998; Irland et al., 2001; Alig et al., 2004). At the same time, forest densification of forest lands under a warming climate may provide conditions of increased wildfire potential (Y. Liu et al., 2013).

5 Conclusions

We assessed the impacts of future climate change on hydrological cycle and ecosystem productivity over the CONUS by linking an ecohydrology model (i.e., WaSSI) with WRF dynamically downscaled the HadCM3 model climate data under the IPCC SRES A2 emission scenario. The current study represents a coupling of bias-corrected, dynamically downscaled climate data with an ecohyrological model to address regional ecosystem issues. The study provides a potential scenario of likely impacts of future climate change on watershed hydrology and productivity across the CONUS, including 82 773 12-digit HUC watersheds. Although only one future climate scenario (the SRES A2 emission scenario) and one GCM (HadCM3 model) was employed here, the methodology applies to other scenarios when more climate change scenarios generated from WRF are available.

Future climate change will not likely change the overall spatial patterns of precipitation, temperature, ET, Q and GPP. However, a large spatial variability in the hydrological and ecosystem productivity responses is expected at both the 12-digit and 2-digit HUC scales. The assessment results provide a benchmark of water yield and ecosystem productivity response across the CONUS. This type of information will be useful for prioritizing watershed restoration and developing specific measures to mitigate the negative impacts of future climate to sustain the terrestrial ecosystem on different spatial scales (i.e., 12-digit HUC and WRR).

Acknowledgements. This study was funded by the National Science Foundation EaSM program (AGS-1049200) with a grant award to North Carolina State University, and the Eastern Forest Environment Threat Assessment Center (EFETAC), USDA Forest Service; and the Nat-

HESSD
12, 12703–12746, 2015

ural Science Foundation of Jiangsu Province, China (BK20151525 and BK20130987). Thanks are due to Francina Dominguez, the University of Illinois, Urbana, Illinois (previously at the University of Arizona, Tucson, Arizona), who provided the WRF simulation data. Thanks are also due to Kai Wang, Changjie Cai, and Xin Li, Air Quality Forecasting Laboratory, NCSU, for processing temperature and precipitation data simulated by WRF into a format needed for WaSSI model.

References

Adams, H. D., Luce, C. H., Breshears, D. D., Allen, C. D., Weiler, M., Hale, V. C., Smith, A. M. S., and Huxman, T. E.: Ecohydrological consequences of drought- and infestation-triggered tree die-off: insights and hypotheses, Ecohydrology, 5, 145–159, 2012.

Aghakouchak, A., Cheng, L., Mazdiyasni, O., and Farahmand, A.: Global warming and changes in risk of concurrent climate extremes: Insights from the 2014 California drought, Geophys. Res. Lett., 41, 8847–8852, 2014.

Alig, R. J., Adams, D., Joyce, L., and Sohngen, B.: Climate change impacts and adaptation in forestry: responses by trees and markets, Choices, 19, 1–7, 2004.

Alkama, R., Marchand, L., Ribes, A., and Decharme, B.: Detection of global runoff changes: results from observations and CMIP5 experiments, Hydrol. Earth Syst. Sci., 17, 2967–2979, 2013, http://www.hydrol-earth-syst-sci.net/17/2967/2013/.

Allen, C. D., Macalady, A. K., Chenchouni, H., Bachelet, D., McDowell, N., Vennetier, M., Kitzberger, T., Rigling, A., Breshears, D. D., Hogg, E. H., Gonzalez, P., Fensham, R., Zhang, Z., Castro, J., Demidova, N., Lim, J. H., Allard, G., Running, S. W., Semerci, A., and Cobb, N.: A global overview of drought and heat induced tree mortality reveals emerging climate change risks for forests, Forest and Ecology and Management, 259, 660–684, 2010.

Anderegg, W. R. L., Berry, J. A., Smith, D. D., Sperry, J. S., Anderegg, L. D. L., and Field, C. B.: The roles of hydraulic and carbon stress in a widespread climate-induced forest die-off. P. Natl. Acad. Sci. USA, 109, 233–237, 2012.

Anderson, B. T., Gianotti, D., and Salvucci, G.: Detectability of historical trends in station-based precipitation characteristics over the continental United States. J. Geophys. Res., 120, 4842–4859, 2015.
Anderson-Teixeira, K. J., Delong, J. P., Fox, A. M., Brese, D. A., and Litvak, M. E.: Differential responses of production and respiration to temperature and moisture drive the carbon balance across a climatic gradient in New Mexico, Glob. Change Biol., 17, 410–424, 2011.
Aparício, S., Carvalhais, N., and Seixas, J.: Climate change impacts on the vegetation carbon cycle of the Iberian Peninsula-Intercomparison of CMIP5 results. J. Geophys. Res., 120, 641–660, 2015.
Arnell, N. W.: Climate change and global water resources, Global Environ. Chang., 9, S31–S49, 1999.
Averyt, K., Meldrum, J., Caldwell, P. V., Sun, G., McNulty, S. G., Huber-Lee, A., and Madden, N.: Sectoral vulnerabilities to changing water resources in the conterminous US, Environ. Res. Lett., 8, 035046, doi:10.1088/1748-9326/8/3/035046, 2013.
Ayres, M. P. and Lombardero, M. J.: Assessing the consequences of climate change for forest herbivore and pathogens, Sci. Total Environ., 262, 263–286, 2000.
Betts, R. A., Boucher, O., Collins, M., Cox, P. M., Falloon, P. D., Gedney, N., Hemming, D. L., Huntingford, C., Jones, C. D., Sexton, D. M. H., and Webb, M. J.: Projected increase in continental runoff due to plant responses to increasing carbon dioxide, Nature, 448, 1037–1041, 2007.
Blanc, E., Strzepek, K., Schlosser, A., Jacoby, H., Gueneau, A., Fant, C., Rausch, S., and Reilly, J.: Modeling US water resources under climate change, Earth's Future, 2, 197–224, 2014.
Bond-Lamberty, B. E. N., Peckham, S. D., Gower, S. T., and Ewers, B. E.: Effects of fire on regional evapotranspiration in the central Canadian boreal forest, Glob. Change Biol., 15, 1242–1254, 2009.
Bony, S., Bellon, G., Klocke, D., Sherwood, S., Fermepin, S., and Denvil, S.: Robust direct effect of carbon dioxide on tropical circulation and regional precipitation, Nat. Geosci., 6, 447–451, 2013.
Brikowski, T. H.: Applying multi-parameter runoff elasticity to assess water availability in a changing climate: an example from Texas, USA, Hydrol. Process., 29, 1746–1756, 2014.
Brookhouse, M. T., Farquhar, G. D., and Roderick, M. L.: The impact of bushfires on water yield from south-east Australia's ash forests, Water Resour. Res., 49, 4493–4505, 2013.

Brown, T. C., Foti, R., and Ramirez, J. A.: Projected freshwater withdrawals in the United States under a changing climate, Water Resour. Res., 49, 1259–1276, 2013.
Burnash, R. J. C.: The NWS river forecast system-catchment modeling, in: Computer Models of Watershed Hydrology, edited by: Singh, V. P., Water Resources Publications, Littleton, Colorado, 311–366, 1995.
Caldwell, P. V., Sun, G., McNulty, S. G., Cohen, E. C., and Moore Myers, J. A.: Impacts of impervious cover, water withdrawals, and climate change on river flows in the conterminous US, Hydrol. Earth Syst. Sci., 16, 2839–2857, doi:10.5194/hess-16-2839-2012, 2012.
Chen, F. and Dudhia, J.: Coupling an advanced land surface–hydrology model with the Penn State–NCAR MM5 modeling system, Part I: Model implementation and sensitivity, Mon. Weather Rev., 129, 569–585, 2001.
Chien, H., Yeh, P. J. F., and Knouft, J. H.: Modeling the potential impacts of climate change on streamflow in agricultural watersheds of the Midwestern United States. J. Hydrol., 491, 73–88, 2013.
Chou, M. D. and Suarez, M. J.: An Efficient Thermal Infrared Radiation Parameterization for Use in General Circulation Models, NASA Technical Memorandum 104606, Technical Report Series on Global Modeling and Data Assimilation, Vol. 3, National Aeronautics and Space Administration, Greenbelt, MD, USA, 85 pp., 1994.
Cook, E. R., Seager, R., Cane, M. A., and Stahle, D. W.: North American drought: Reconstructions, causes, and consequences, Earth-Sci. Rev., 81, 93–134, 2007.
Cox, P. M., Betts, R. A., Jones, C. D., Spall, S. A., and Totterdell, I. J.: Acceleration of global warming due to carbon-cycle feedbacks in a coupled climate model, Nature, 408, 184–187, 2000.
Dai, A., Qian, T., Trenberth, K. E., and Milliman, J. D.: Changes in continental freshwater discharge from 1948 to 2004. J. Climate, 22, 2773–2792, 2009.
Daly, C., Neilson, R. P., and Phillips, D. L.: A statistical topographic model for mapping climatological precipitation over mountainous terrain. J. Appl. Meteorol., 33, 140–158, 1994.
DeRose, R. J. and Long, J. N.: Drought-driven disturbance history characterizes a southern Rocky Mountain subalpine forest, Can. J. Forest Res., 42, 1649–1660, 2012.
Dolbeth, M., Martinho, F., Viegas, I., Cabral, H., and Pardal, M. A.: Estuarine production of resident and nursery fish species: conditioning by drought events?, Estuar. Coast. Shelf S., 78, 51–60, 2008.

HESSD
12, 12703–12746, 2015
Predicting future US water yield and ecosystem productivity
S. Sun et al.

Dominguez, F., Cañon, J., and Valdes, J.: IPCC-AR4 climate simulations for the Southwestern US: the importance of future ENSO projections, Climatic Change, 99, 499–514, 2009.
Dore, S., Kolb, T. E., Montes-Helu, M., Eckert, S. E., Sullivan, B. W., Hungate, B. A., Kaye, J. P., Hart, S. C., Koch, G. W., and Finkral, A.: Carbon and water fluxes from ponderosa pine forests disturbed by wildfire and thinning, Ecol. Appl., 20, 663–683, 2010.
Foley, J. A., Defries, R., Asner, G. P., Barford, C., Bonan, G., Carpenter, S. R., Chapin, F. S., Coe, M. T., Daily, G. C., Gibbs, H. K., Helkowski, J. H., Holloway, T., Howard, E. A., Kucharik, C. J., Monfreda, C., Patz, J. A., Prentice, I. C., Ramankutty, N., and Snyder, P. K.: Global consequences of land use, Science, 309, 570–574, 2005.
Fry, J., Xian, G., Jin, S., Dewitz, J., Homer, C., Yang, L., Barnes, C., Herold, N., and Wickham, J.: Completion of the 2006 National Land Cover Database for the conterminous United States. Photogramm. Eng. Rem. S., 77, 858–864, 2011.
Gang, C., Zhou, W., Li, J., Chen, Y., Mu, S., Ren, J., Chen, J., and Groisman, P. Y.: Assessing the spatiotemporal variation in distribution, extent and NPP of terrestrial ecosystems in response to climate change from 1911 to 2000. PLoS One, 8, e80394, doi:10.1371/journal.pone.0080394, 2013.
Gao, Y., Vano, J. A., Zhu, C., and Lettenmaier, D. P.: Evaluating climate change over the Colorado River basin using regional climate models. J. Geophys. Res., 116, D13104, doi:10.1029/2010jd015278, 2011.
Gedney, N., Cox, P. M., Betts, R. A., Boucher, O., Huntingford, C., and Stott, P. A.: Detection of a direct carbon dioxide effect in continental river runoff records, Nature, 439, 835–838, 2006.
Gillson, J., Scandol, J., and Suthers, L.: Estuarine gillnet fishery catch rates decline during drought in eastern Australia, Fish. Res., 99, 26–37, 2009.
Groisman, P. Y., Knight, R. W., and Karl, T. R.: Heavy precipitation and high streamflow in the contiguous United States: trends in the twentieth century, B. Am. Meteorol. Soc., 82, 219–246, 2001.
Groisman, P. Y., Knight, R. W., Karl, T. R., Easterling, D. R., Sun, B., and Lawrimore, J. H.: Contemporary changes of the hydrological cycle over the contiguous United States: Trends derived from in situ observations, J. Hydrometeorol., 5, 64–85, 2004.
Guardiola-Claramonte, M., Troch, P. A., Breshears, D. D., Huxman, T. E., Switanek, M. B., Durcik, M., and Cobb, N. S.: Decreased streamflow in semi-arid basins following drought-induced tree die-off: a counter-intuitive and indirect climate impact on hydrology, J. Hydrol., 406, 225–233, 2011.

HESSD
12, 12703–12746, 2015

Predicting future US water yield and ecosystem productivity

S. Sun et al.

Hamlet, A. F., Mote, P. W., Clark, M. P., and Lettenmaier, D. P.: Twentieth-century trends in runoff, evapotranspiration, and soil moisture in the western United States, J. Climate, 20, 1468–1486, 2007.

Hanson, P. J. and Weltzin, J. F.: Drought disturbance from climate change: response of United States forests, Sci. Total Environ., 262, 205–220, 2000.

Harding, R., Best, M., Blyth, E., Hagemann, S., Kabat, P., Tallaksen, L. M., Warnaars, T., Wiberg, D., Weedon, G. P., van Lanen, H., Ludwig, F., and Haddeland, I.: WATCH: current knowledge of the terrestrial global water cycle, J. Hydrometeorol., 12, 1149–1156, 2011.

Hegerl, G. C., Black, E., Allan, R. P., Ingram, W. J., Polson, D., Trenberth, K. E., Chadwick, R. S., Arkin, P. A., Sarojini, B. B., Becker, A., Dai, A., Durack, P. J., Easterling, D., Fowler, H. J., Kendon, E. J., Huffman, G. J., Liu, C., Marsh, R., New, M., Osbornm, T. J., Skliris, N., Stotto, P. A., Vidale, P.-L., Wijffels, S. E., Wilcox, L. J., and Zhang, X.: Challenges in quantifying changes in the global water cycle, B. Am. Meteorol. Soc., 96, 1097–1115, doi:10.1175/bams-d-13-00212.1, 2014. ater Cycle. Bull. Amer. Meteor. Soc..

Hong, S.-Y., Dudhia, J., and Chen, S.-H.: A revised approach to ice microphysical processes for the bulk parameterization of clouds and precipitation, Mon. Weather Rev., 132, 103–120, 2004.

Hu, W. W., Wang, G. X., Deng, W., and Li, S. N.: The influence of dams on ecohydrological conditions in the Huaihe River basin, China, Ecol. Eng., 33, 233–241, 2008.

Huang, J., Zhang, J., Zhang, Z., Sun, S., and Yao, J.: Simulation of extreme precipitation indices in the Yangtze River basin by using statistical downscaling method (SDSM), Theor. Appl. Climatol., 108, 325–343, 2011.

Huntington, T. G. and Billmire, M.: Trends in precipitation, runoff, and evapotranspiration for rivers draining to the Gulf of Maine in the United States, J. Hydrometeorol., 15, 726–743, 2014.

Ingjerd, H., Jens, H., Hester, B., Stephanie, E., Martina, F., Naota, H., Markus, K., Fulco, L., Yoshimitsu, M., Jacob, S., Tobias, S., Zachary, D. T.,Yoshihide, W., and Dominik, W.: Global water resources affected by human interventions and climate change, P. Natl. Acad. Sci. USA, 111, 3251–3256, 2014.

IPCC: Summary for policymakers, in: Climate Change 2014, Impacts, Adaptation, and Vulnerability, Part A: Global and Sectoral Aspects, Contribution of Working Group II to the Fifth Assessment Report of the Intergovernmental Panel on Climate Change, edited by: Field, C. B., Barros, V. R., Dokken, D. J., Mach, K. J., Mastrandrea, M. D., Bilir, T. E., Chatterjee, M.,

Ebi, K. L., Estrada, Y. O., Genova, R. C., Girma, B., Kissel, E. S., Levy, A. N., MacCracken, S., Mastrandrea, P. R., and White, L. L., Cambridge University Press, Cambridge, UK and New York, NY, USA, 1–32, 2014.
Irland, L., Adams, D., Alig, R., Betz, C., Chen, C., Hutchins, M., McCarl, B., Skog, K., and Sohngen, B.: Assessing socioeconomic impacts of climate change on US forests, wood-product markets, and forest recreation, Bioscience, 51, 753–764, 2001.
Jactel, H., Petit, J., Desprez-Loustau, M.-L., Delzon, S., Piou, D., Battisti, A., and Koricheva, J.: Drought effects on damage by forest insects and pathogens: a meta-analysis, Glob. Change Biol., 18, 267–276, 2012.
Janjic, Z. I.: Nonsingular implementation of the Mellor-Yamada level 2.5 scheme in the NCEP meso-model, NCEP Office Note no. 437, 61 pp., National Centers for Environmental Prediction, Camp Springs, Maryland, 2002.
Joseph, R. and Nigam, S.: ENSO evolution and teleconnections in IPCC's twentieth-century climate simulations: realistic representation, J. Climate, 19, 4360–4377, 2006.
Kain, J. S. and Fritsch, J. M.: Convective parameterization for mesoscale models: the Kain–Fritsch scheme, in: The Representation of Cumulus Convection in Numerical Models, edited by: Emanuel, K. A., and Raymond, D. J., American Meteorological Society, Boston, 165–170, 1993.
Kundzewicz, Z. W. and Gerten, D. G.: Challenges related to the assessment of climate change impacts on freshwater resources, J. Hydrol. Eng., 20, A4014011, doi:10.1061/(asce)he.1943-5584.0001012, 2015.
Labat, D., Goddéris, Y., Probst, J. L., and Guyot, J. L.: Evidence for global runoff increase related to climate warming, Adv. Water Resour., 27, 631–642, 2004.
Lee, C., Schlemme, C., Murray, J., and Unsworth, R.: The cost of climate change: Ecosystem services and wildland fires, Ecol. Econ., 116, 261–269, 2015.
Lenihan, J. M., Bachelet, D., Neilson, R. P., and Drapek, R.: Simulated response of conterminous United States ecosystems to climate change at different levels of fire suppression, CO_2 emission rate, and growth response to CO_2, Global Planet. Change, 64, 16–25, 2008.
Lettenmaier, D. P., Wood, E. F., and Wallis, J. R.: Hydro-climatological trends in the continental United States, 1948–88, J. Climate, 7, 586–607, 1994.
Leung, L. R. and Qian, Y.: The sensitivity of precipitation and snowpack simulations to model resolution via nesting in regions of complex terrain, J. Hydrometeorol., 4, 1025–1043, 2003.

HESSD
12, 12703–12746, 2015

Li, H., Huang, M., Wigmosta, M. S., Ke, Y., Coleman, A. M., Leung, L. R., Wang, A., and Ricciuto, D. M.: Evaluating runoff simulations from the Community Land Model 4.0 using observations from flux towers and a mountainous watershed, J. Geophys. Res., 116, D24120, doi:10.1029/2011jd016276, 2011.

Lins, H. F. and Slack, J. R.: Streamflow trends in the United States, Geophys. Res. Lett., 26, 227–230, 1999.

Liu, J., Wang, B., Cane, M. A., Yim, S.-Y., and Lee, J.-Y.: Divergent global precipitation changes induced by natural versus anthropogenic forcing, Nature, 493, 656–659, 2013.

Liu, N., Sun, P., Liu, S., and Sun, G.: Coupling simulation of water–carbon processes for catchment: calibration and validation of the WaSSI-C model, Chinese J. Plant Ecol.-UK, 37, 492–502, 2013. (in Chinese with English abstract)

Liu, Y., Prestemon, J., Goodrick, S., Holmes, T., Stanturf, J., Vose, J., and Sun, G.: Chapter 5: Future Wildfire Trends, Impacts, and Mitigation Options in the Southern United States, in: Climate Change Adaptation and Mitigation Management Options, edited by: Vose, J. and Klepzig, K. D., CRS Press, Boca Raton London New York, p. 476, 2013.

Lockaby, G., Nagy, C., Vose, J. M., Ford, C. R., Sun, G., McNulty, S. G., Caldwell, P. V., Cohen, E., and Moore Myers, J. A.: Water and forests, in: The Southern Forest Futures Project: Technical Report, edited by: Wear, D. N. and Greis, J. G., General Technical Report, USDA Forest Service, Southern Research Station, Asheville, NC, 2011.

Magoulick, D. D. and Kobza, R. M.: The role of refugia for fishes during drought: a review and synthesis, Freshwater Biol., 48, 1186–1198, 2003.

Mao, Y., Nijssen, B., and Lettenmaier, D. P.: Is climate change implicated in the 2013–2014 California drought? A hydrologic perspective, Geophys. Res. Lett., 42, 2805–2813, 2015.

Marengo, J. A., Tomasella, J., Cardoso, M. F., and Oyama, M. D.: Hydro-climatic and ecological behaviour of the drought of Amazonia in 2005. Philos. T. R. Soc. B, 363, 1773–1778, 2008.

Marion, D. A., Sun, G., Caldwell, P. V., Miniat, C. F., Ouyang, Y., Amatya, D. M., Clinton, B. D., Conrads, P. A., Gull Laird, S., Dai, Z., Clingenpeel, J. A., Liu, Y., Roehl Jr., E. A., Myers, J. A. M., and Trettin, C.: Managing forest water quantity and quality under climate change, in: Climate Change Adaptation and Mitigation Management Options: A Guide for Natural Resource Managers in Southern Forest Ecosystems, edited by: Vose, J. M. and Klepzig, K. D., CRC Press, Boca Raton, FL, 249–305, 2014.

McCabe, G. J.: A step increase in streamflow in the conterminous United States. Geophys. Res. Lett., 29, 2185, doi:10.1029/2002gl015999, 2002.

McCabe, G. J. and Markstrom, S. L.: A Monthly Water-Balance Model Driven by a Graphical User Interface, U.S. Geological Survey Open-File report 2007–1088, 6 pp., US Geological Survey, Reston, Virginia, 2007.

McCabe, G. J. and Wolock, D. M.: Future snowpack conditions in the western United States derived from general circulation model climate simulations, J. Am. Water Resour. As., 35, 1473–1484, 1999.

McCabe, G. J. and Wolock, D. M.: Independent effects of temperature and precipitation on modeled runoff in the conterminous United States, Water Resour. Res., 47, W11522, doi:10.1029/2011wr010630, 2011.

McCabe, G. J. and Wolock, D. M.: Spatial and temporal patterns in conterminous United States streamflow characteristics, Geophys. Res. Lett., 41, 6889–6897, 2014.

McNulty, S. G., Cohen, E. C., Sun, G., and Caldwell, P.: Chapter 1.7: Hydrologic modelling for water resource assessment in a developing country: the Rwanda case study, in: Watershed Modeling, edited by: Lafforgue, M., in press, 2015.

Meehl, G. A., Arblaster, J. M., and Tebaldi, C.: Understanding future patterns of increased precipitation intensity in climate model simulations, Geophys. Res. Lett., 32, L18719, doi:10.1029/2005gl023680, 2005.

Meehl, G., Covey, C., Delworth, T., Latif, M., McAvaney, B., Mitchell, J., Stouffer, R., and Taylor, K.: The WCRP CMIP3 multi-model dataset. A new era in climate change research, B. Am. Meteorol. Soc., 88, 1383–1394, 2007.

Milly, P. C., Dunne, K. A., and Vecchia, A. V.: Global pattern of trends in streamflow and water availability in a changing climate, Nature, 438, 347–350, 2005.

Mlawer, E. J., Taubman, S. J., Brown, P. D., Iacono, M. J., and Clough, S. A.: Radiative transfer for inhomogeneous atmospheres: RRTM, a validated correlated-k model for the longwave, J. Geophys. Res., 102, 16663, doi:10.1029/97jd00237, 1997.

Myneni, R. B., Keeling, C. D., Tucker, C. J., Asrar, G., and Nemani, R. R.: Increased plant growth in the northern high latitudes from 1981 to 1991, Nature, 386, 698–702, 1997.

Nakicenvoic, N. and Swart, R.: Special report on emissions scenarios, a special report of Working Group III of the Intergovernmental Panel on Climate Change, Cambridge University Press, Cambridge, 599 pp., 2000.

National Research Council: Estimating Water Use in the United States – A New Paradigm for the National Water Use Information Program, The National Academies Press, Washington, DC, 176 pp., 2002.

HESSD
12, 12703–12746, 2015

Predicting future US water yield and ecosystem productivity

S. Sun et al.

Title Page
Abstract Introduction
Conclusions References
Tables Figures
◀◀ ▶▶
◀ ▶
Back Close
Full Screen / Esc
Printer-friendly Version
Interactive Discussion

Nemani, R. R., Keeling, C. D., Hashimoto, H., Jolly, W. M., Piper, S. C., Tucker, C. J., Myneni, R. B., and Running, S. W.: Climate-driven increases in global terrestrial net primary production from 1982 to 1999, Science, 300, 1560–1563, 2003.
Neary, D. G., Ryan, K. C., DeBano, L. F. (eds.): Wildland Fire in Ecosystems: Effects of Fire on Soil and Water, Gen. Tech. Rep. RMRS-GTR-32-vol. 4. U.S. Department of Agriculture, Forest Service, Rocky Mountain Research Station, Ogden, UT, 250 p, 2005.
Noake, K., Polson, D., Hegerl, G., and Zhang, X.: Changes in seasonal land precipitation during the latter twentieth-century, Geophys. Res. Lett., 39, L03706, doi:10.1029/2011gl050405, 2012.
Nolan, R. H., Lane, P. N. J., Benyon, R. G., Bradstock, R. A., and Mitchell, P. J.: Changes in evapotranspiration following wildfire in resprouting eucalypt forests, Ecohydrology, 7, 1363–1377, 2014.
Oki, T. and Kanae, S.: Global hydrological cycles and world water resources, Science, 313, 1068–1072, 2006.
Overgaard, J., Rosbjerg, D., and Butts, M. B.: Land-surface modelling in hydrological perspective – a review, Biogeosciences, 3, 229–241, 2006, http://www.biogeosciences.net/3/229/2006/.
Overpeck, J. T., Rind, D., and Goldberg, R.: Climate-induced changes in forest disturbance and vegetation, Nature, 343, 51–53, 1990.
Peng, S., Piao, S., Ciais, P., Myneni, R. B., Chen, A., Chevallier, F., Dolman, A. J., Janssens, I. A., Peñuelas, J., Zhang, G., Vicca, S., Wan, S., Wang, S., and Zeng, H.: Asymmetric effects of daytime and night-time warming on Northern Hemisphere vegetation, Nature, 501, 88–92, 2013.
Pennington, D. D. and Collins, S. L.: Response of an aridland ecosystem to interannual climate variability and prolonged drought, Landscape Ecology, 22, 897–910, 2007.
Piao, S., Friedlingstein, P., Ciais, P., de Noblet-Ducoudre, N., Labat, D., and Zaehle, S.: Changes in climate and land use have a larger direct impact than rising CO_2 on global river runoff trends. P. Natl. Acad. Sci. USA, 104, 15242–15247, 2007.
Piao, S., Yin, G., Tan, J., Cheng, L., Huang, M., Li, Y., Liu, R., Mao, J., Myneni, R. B., Peng, S., Poulter, B., Shi, X., Xiao, Z., Zeng, N., Zeng, Z., and Wang, Y.: Detection and attribution of vegetation greening trend in China over the last 30 years. Glob. Change Biol., 21, 1601–1609, 2015.

Piontek, F., Muller, C., Pugh, T. A., Clark, D. B., Deryng, D., Elliott, J., de Jesus Colón Gonzálezf, F., Flörke, M., Folberth, C., Franssen, W., Frieler, K., Friend, A. D., Gosling, S. N., Hemming, D., Khabarov, N., Kim, H., Lomas, M. R., Masaki, Y., Mengel, M., Morse, A., Neuman, K., Nishina, K., Ostberg, S., Pavlick, R., Ruane, A. C., Schewe, J., Schmid, E., Stacke, T., Tang, Q., Tessler, Z. D., Tompkins, A. M., Warszawski, L., Wisser, D., and Schellnhuber, H. J.: Multisectoral climate impact hotspots in a warming world. P. Natl. Acad. Sci. USA, 111, 3233–3238, 2014.

PRISM Climate Group: Descriptions of PRISM spatial climate datasets for the conterminous United States, available at: http://www.prism.oregonstate.edu/documents/PRISM_datasets_aug2013.pdf, 2013.

Qi, S., Sun, G., Wang, Y., McNulty, S. G., and Moore, M. J. A.: Streamflow response to climate and landuse changes in a coastal watershed in North Carolina, Trans. Am. Soc. Agric. Engin., 52, 739–749, 2009.

Raupach, M. R., Marland, G., Ciais, P., Le Quéré, C., Canadell, J. G., Klepper, G., and Field, C. B.: Global and regional drivers of accelerating CO_2 emissions, P. Natl. Acad. Sci. USA, 104, 10288–10293, 2007.

Reichstein, M., Bahn, M., Ciais, P., Frank, D., Mahecha, M. D., Seneviratne, S., Zscheischler, J., Beer, C., Buchmann, N., Frank, D. C., Papale, D., Rammig, A., Smith, P., Thonicke, K., van der Velde, M., Vicca, S., Walz, A., and Wattenbach, M.: Climate extremes and the carbon cycle, Nature, 500, 287–295, 2013.

Roberts, T.: Downstream Ecological Implications of China's Lancang Hydropower and Mekong Navigation Project, available at: http://www.internationalrivers.org/files/attached-files/tyson_roberts_paper_on_yunnan.pdf (last access: 5 December 2015)„ 2001.

Sagarika, S., Kalra, A., and Ahmad, S.: Evaluating the effect of persistence on long-term trends and analyzing step changes in streamflows of the continental United States, J. Hydrol., 517, 36–53, 2014.

Sankarasubramanian, A.: Hydroclimatology of the continental United States. Geophys. Res. Lett., 30, 1363, doi:10.1029/2002gl015937, 2003.

Sankarasubramanian, A., Vogel, R. M., and Limbrunner, J. F.: Climate elasticity of streamflow in the United States. Water Resour. Res., 37, 1771–1781, 2001.

Scheff, J. and Frierson, D. M. W.: Robust future precipitation declines in CMIP5 largely reflect the poleward expansion of model subtropical dry zones, Geophys. Res. Lett., 39, L18704, doi:10.1029/2012gl052910, 2012.

Schewe, J., Heinke, J., Gerten, D., Haddeland, I., Arnell, N. W., Clark, D. B., Dankers, R., Eisner, S., Fekete, B. M., Colón-González, F. J., Gosling, S. N., Kim, H., Liu, X., Masaki, Y., Portman, F. T., Satoh, Y., Stacke, T., Tang, Q., Wada, Y., Wisser, D., Albrecht, T., Frieler, K., Piontek, F., Warszawski, L., and Kabat, P.: Multimodel assessment of water scarcity under climate change, P. Natl. Acad. Sci. USA, 111, 3245–3250, 2014.

Schilling, K. E., Jha, M. K., Zhang, Y.-K., Gassman, P. W., and Wolter, C. F.: Impact of land use and land cover change on the water balance of a large agricultural watershed: Historical effects and future directions, Water Resour. Res., 44, W00A09, doi:10.1029/2007wr006644, 2008.

Schoeneweiss, D. F.: The role of environmental stress in diseases of woody plants, Plant Disease, 65, 308–314, 1981.

Scholze, M., Knorr, W., Arnell, N. W., and Prentice, I. C.: A climate-change risk analysis for world ecosystems. P. Natl. Acad. Sci. USA, 103, 13116–13120, 2006.

Seaber, P. R., Kapinos, F. P., and Knapp, G. L.: Hydrologic Unit Maps, Water Supply Paper 2294, US Government Printing Office, Washington, DC, 1987.

Sedláček, J. and Knutti, R.: Half of the world's population experience robust changes in the water cycle for a 2 °C warmer world, Environ. Res. Lett., 9, 044008, doi:10.1088/1748-9326/9/4/044008, 2014.

Sitch, S., Huntingford, C., Gedney, N., Levy, P. E., Lomas, M., Piao, S. L., Betts, R., Ciais, P., Cox, P., Friedlingstein, P., Jones, C. D., Prentice, I. C., and Woodward, F. I.: Evaluation of the terrestrial carbon cycle, future plant geography and climate-carbon cycle feedbacks using five Dynamic Global Vegetation Models (DGVMs). Glob. Change Biol., 14, 2015–2039, 2008.

Skamarock, W. C., Klemp, J. B., Dudhia, J., Gill, G. O., Barker, D. M., Wang, W., and Powers, J. G.: A description of the advanced research WRF version 2, TN-468+STR, NCAR Technical Note, Mesoscale and Microscale Meteorology Division, National Center for Atmospheric Research, Boulder, Colorado, USA, 100 pp., 2005.

Sohngen, B. and Mendelsohn, R.: Valuing the impact of large-scale ecological change in a market: the effect of climate change on US timber, Am. Econ. Rev., 88, 686–710, 1998.

Somerville, C. and Briscoe, J.: Genetic engineering and water, Science, 292, 2217, doi:10.1126/science.292.5525.2217, 2001.

Sun, G., McNulty, S. G., Myers, J. A. M., and Cohen, E.: Impacts of multiple stresses on water demand and supply across the southeastern United States. J. Am. Water Resour. As., 44, 1441–1457, 2008.

HESSD
12, 12703–12746, 2015

Sun, G., Alstad, K., Chen, J., Chen, S., Ford, C. R., Lin, G., Liu, C., Lu, N., McNulty, S. G., Miao, H., Noormets, A., Vose, J. M., Wilske, B., Zeppel, M., Zhang, Y., and Zhang, Z.: A general predictive model for estimating monthly ecosystem evapotranspiration, Ecohydrology, 4, 245–255, 2011a.

Sun, G., Caldwell, P., Noormets, A., Cohen, E., McNulty, S., Treasure, E., Domec, J. C., Mu, Q., Xiao, J., John, R., and Chen, J.: Upscaling key ecosystem functions across the conterminous United States by a water-centric ecosystem model, J. Geophys. Res., 116, G00J05, doi:10.1029/2010JG001573, 2011b.

Sun, S., Chen, H., Ju, W., Yu, M., Hua, W., and Yin, Y.: On the attribution of the changing hydrological cycle in Poyang Lake Basin, China. J. Hydrol., 514, 214–225, 2014.

Sun, S., Sun, G., Caldwell, P., McNulty, S., Cohen, E., Xiao, J., and Zhang, Y.: Drought impacts on ecosystem functions of the US National Forests and Grasslands: Part II Assessment results and management implications, Forest Ecol. Manag., 353, 269–279, 2015a.

Sun, S., Sun, G., Caldwell, P., McNulty, S. G., Cohen, E., Xiao, J., and Zhang, Y.: Drought impacts on ecosystem functions of the US National Forests and Grasslands: Part I Evaluation of a water and carbon balance model, Forest Ecol. Manag., 353, 260–268, 2015b.

Syed, T. H., Famiglietti, J. S., Chambers, D. P., Willis, J. K., and Hilburn, K.: Satellite-based global-ocean mass balance estimates of interannual variability and emerging trends in continental freshwater discharge, P. Natl. Acad. Sci. USA, 107, 17916–17921, 2010.

Tavernia, B. G., Nelson, M. D., Caldwell, P. V., and Sun, G.: Water stress projections for the northeastern and midwestern United States in 2060: Anthropogenic and ecological consequences, J. Am. Water Resour. As., 49, 938–952, 2013.

Tebaldi, C., Hayhoe, K., Arblaster, J. M., and Meehl, G. A.: Going to the extremes: an intercomparison of model-simulated historical and future changes in extreme events, Climatic Change, 79, 185–211, 2006.

Theiling, C. H., Maher, R. J., and Sparks, R. E.: Effects of variable annual hydrology on a river regulated for navigation: Pool 26, Upper Mississippi River System, J. Freshw. Ecol., 11, 101–114, 1996.

Thomas, D. S. K., Wilhelmi, O. V., Finnessey, T. N., Deheza, V., and Sun, J.: A comprehensive framework for tourism and recreation drought vulnerability reduction, Environ. Res. Lett., 8, 575–591, 2013.

HESSD
12, 12703–12746, 2015

Thompson, J. R., Foster, D. R., Scheller, R., and Kittredge, D.: The influence of land use and climate change on forest biomass and composition in Massachusetts, USA. Ecol. Appl., 21, 2425–2444, 2011.
Trenberth, K. E.: Changes in precipitation with climate change, Clim. Res., 47, 123–138, 2011.
van Oldenborgh, G. J., Philip, S. Y., and Collins, M.: El Niño in a changing climate: a multi-model study, Ocean Sci., 1, 81–95, 2005, http://www.ocean-sci.net/1/81/2005/.
Wang, C., Cao, R., Chen, J., Rao, Y., and Tang, Y.: Temperature sensitivity of spring vegetation phenology correlates to within-spring warming speed over the Northern Hemisphere. Ecol. Indic., 50, 62–68, 2015.
Wang, D. and Hejazi, M.: Quantifying the relative contribution of the climate and direct human impacts on mean annual streamflow in the contiguous United States. Water Resour. Res., 47, W00J12, doi:10.1029/2010wr010283, 2011.
Wang, F., Notaro, M., Liu, Z., and Chen, G.: Observed local and remote influences of vegetation on the atmosphere across north America using a model-validated statistical technique that first excludes oceanic forcings, J. Climate, 27, 362–382, 2014.
Watershed Boundary Dataset (WBD): http://www.nrcs.usda.gov/wps/portal/nrcs/main/national/water/watersheds/dataset, 2010.
Wi, S., Dominguez, F., Durcik, M., Valdes, J., Diaz, H. F., and Castro, C. L.: Climate change projection of snowfall in the Colorado River Basin using dynamical downscaling, Water Resour. Res., 48, W05504, doi:10.1029/2011wr010674, 2012.
Williams, I. N., Torn, M. S., Riley, W. J., and Wehner, M. F.: Impacts of climate extremes on gross primary production under global warming, Environ. Res. Lett., 9, 094011, doi:10.1088/1748-9326/9/9/094011, 2014.
Wood, A. W.: Long-range experimental hydrologic forecasting for the eastern United States. J. Geophys. Res., 107, 4429, doi:10.1029/2001jd000659, 2002.
Wood, A. W., Leung, L. R., Sridhar, V., and Lettenmaier, D. P.: Hydrologic implications of dynamical and statistical approaches to downscaling climate model outputs, Climatic Change, 62, 189–216, 2004.
Xu, X., Liu, W., Rafique, R., and Wang, K.: Revisiting continental US hydrologic change in the latter half of the 20th century, Water Resour. Manag., 27, 4337–4348, 2013.

Xue, Y., Janjic, Z., Dudhia, J., Vasic, R., and De Sales, F.: A review on regional dynamical downscaling in intraseasonal to seasonal simulation/prediction and major factors that affect downscaling ability, Atmos. Res., 147–148, 68–85, 2014.
Yao, S.: Effects of fire disturbance on forest hydrology. J. Forest. Research, 14, 331–334, doi:10.1007/bf02857863, 2003.
Yu, M., Wang, G., Parr, D., and Ahmed, K. F.: Future changes of the terrestrial ecosystem based on a dynamic vegetation model driven with RCP8.5 climate projections from 19 GCMs. Climatic Change, 127, 257–271, 2014.
Zhang, Y., Song, C., Zhang, K., Cheng, X., Band, L. E., and Zhang, Q.: Effects of land use/land cover and climate changes on terrestrial net primary productivity in the Yangtze River Basin, China, from 2001 to 2010. J. Geophys. Res., 119, 1092–1109, 2014.
Zhang, Y., Moran, M. S., Nearing, M. A., Ponce Campos, G. E., Huete, A. R., Buda, A. R., Bosch, D. D., Gunter, S. A., Kitchen, S. G., McNab, W. H., Morgan, J. A., McClaran, M. P., Montoya, D. S., Peters, D. P. C., and Starks, P. J.: Extreme precipitation patterns and reductions of terrestrial ecosystem production across biomes, J. Geophys. Res., 118, 148–157, doi:10.1029/2012JG002136, 2013.

Table 1. Multi-year mean precipitation, temperature, ET, *Q* and GPP averaged over each WRR or the entire CONUS during the baseline (1979–2007) and the future period (2031–2060).

WRR	Precipitation ($mm\,yr^{-1}$)		Temperature (°C)		ET ($mm\,yr^{-1}$)		*Q* ($mm\,yr^{-1}$)		GPP ($g\,C\,m^{-2}\,yr^{-1}$)	
	Baseline	Future	Baseline	Future	Baseline	Future	Baseline	Future	Baseline	Future
1	1143	1169	6.3	8.0	506	538	636	632	1218	1316
2	1100	1211	10.2	11.8	582	629	518	583	1564	1712
3	1299	1334	17.5	19.2	823	863	477	471	2104	2207
4	875	944	7.3	9.0	476	518	400	427	1241	1376
5	1123	1297	11.6	13.1	580	641	543	655	1680	1882
6	1354	1395	13.8	15.4	769	810	585	585	2218	2347
7	863	931	8.5	10.3	550	597	314	335	1516	1677
8	1414	1425	17.4	19.2	836	877	577	549	2247	2361
9	542	592	4.2	6.5	429	472	115	123	1120	1256
10	534	572	7.9	10.1	424	462	115	118	985	1104
11	819	840	14.0	15.8	593	626	229	219	1502	1597
12	828	866	18.7	20.3	615	650	215	220	1379	1457
13	392	419	13.9	15.7	368	394	35	35	602	651
14	397	411	7.3	9.4	318	343	86	76	546	614
15	342	387	15.1	16.8	316	354	34	40	522	588
16	339	372	8.6	10.8	298	331	54	50	478	557
17	854	841	7.2	9.2	464	481	395	363	904	972
18	626	647	13.9	15.7	366	391	267	258	740	793
CONUS	801	844	11.2	13.1	515	551	290	297	1232	1339

HESSD
12, 12703–12746, 2015

Table 2. Future changes in multi-year mean precipitation, temperature, ET, Q and GPP averaged over each WRR or the entire CONUS relative to the baseline period.

WRR	Precipitation		Temperature	ET		Q		GPP	
	Absolute ($mm\,yr^{-1}$)	Percent (%)	Absolute (°C)	Absolute ($mm\,yr^{-1}$)	Percent (%)	Absolute ($mm\,yr^{-1}$)	Percent (%)	Absolute ($g\,C\,m^{-2}\,yr^{-1}$)	Percent (%)
1	26	2	1.7	32	6	−4	−1	98	8
2	111	10	1.6	46	8	65	13	148	9
3	35	3	1.6	40	5	−7	−1	103	5
4	68	8	1.7	42	9	27	7	135	11
5	174	15	1.6	61	11	113	21	202	12
6	40	3	1.7	41	5	0	0	129	6
7	68	8	1.8	47	9	22	7	160	11
8	11	1	1.8	41	5	−29	−5	114	5
9	50	9	2.2	43	10	8	7	136	12
10	38	7	2.2	39	9	3	3	119	12
11	21	3	1.9	33	6	−10	−4	95	6
12	38	5	1.7	35	6	4	2	78	6
13	26	7	1.8	27	7	1	2	49	8
14	14	4	2.1	25	8	−10	−12	68	13
15	45	13	1.7	39	12	6	16	65	13
16	33	10	2.1	33	11	−3	−6	79	17
17	−13	−1	2.0	18	4	−32	−8	69	8
18	21	3	1.8	25	7	−9	−3	53	7
CONUS	45	6	1.8	37	7	9	3	106	9

HESSD
12, 12703–12746, 2015

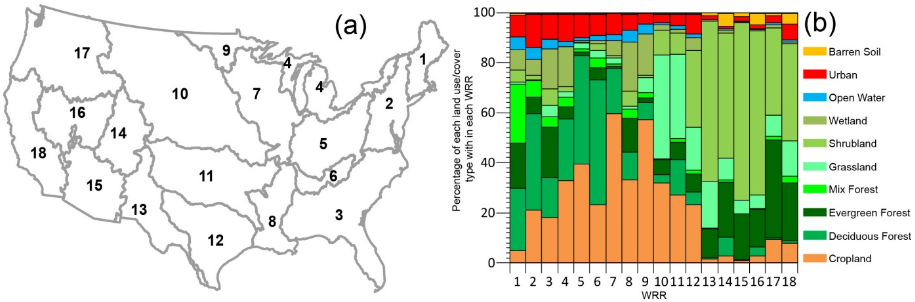

Figure 1. Location of the Water Resource Regions (WRRs) over the CONUS **(a)** with the percentage of each land use/cover type within each WRR. The numeral from 1 to 18 in left of this figure represents the number of WRR. For right figure, the rectangle size notes the percentage of each land use/cover type within each WRR. Note that the percentages of each land use/cover were calculated based on the 2006 National Land Cover Dataset (NLCD) of CONUS.

HESSD
12, 12703–12746, 2015

Title Page
Abstract | Introduction
Conclusions | References
Tables | Figures
◀I | ▶I
◀ | ▶
Back | Close
Full Screen / Esc
Printer-friendly Version
Interactive Discussion

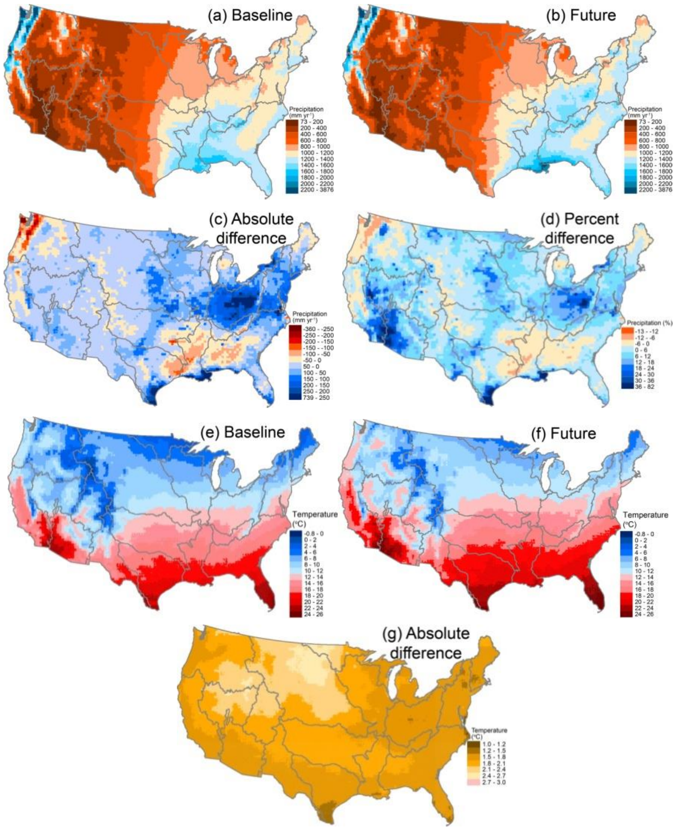

Figure 2. Characteristics of precipitation and temperature during the baseline (1979–2007) and the future (2031–2060) period, and the future changes (future–baseline).

HESSD
12, 12703–12746, 2015

Title Page
Abstract Introduction
Conclusions References
Tables Figures
◀ ▶
◀ ▶
Back Close
Full Screen / Esc
Printer-friendly Version
Interactive Discussion

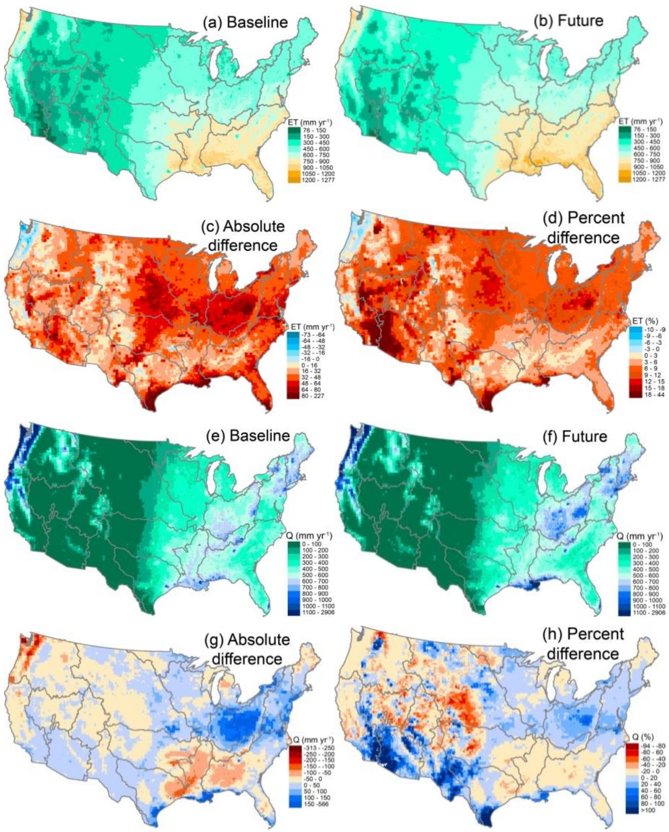

Figure 3. Spatial distribution of ET and Q during the baseline and the future periods, and the future changes.

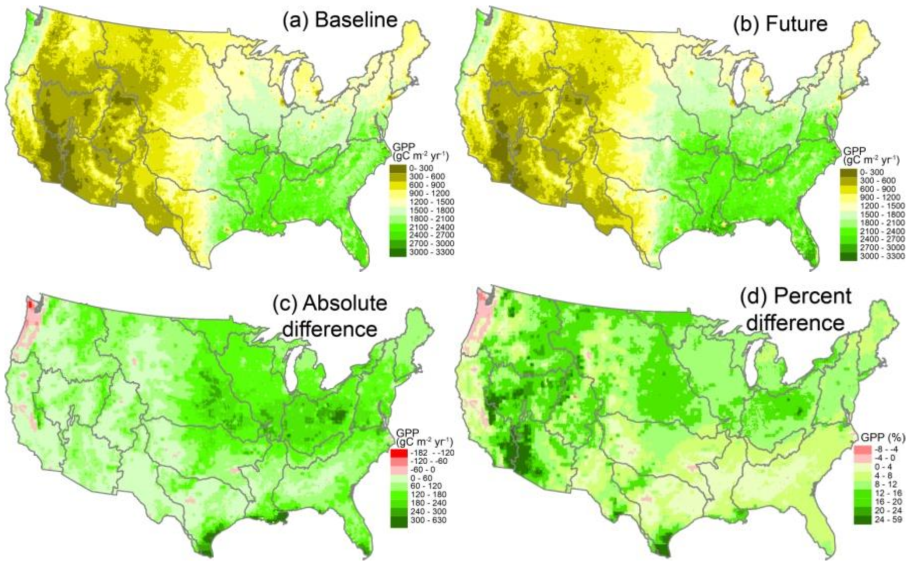

Figure 4. Spatial distribution of GPP during the baseline and the future periods, and climate change impacts (future–baseline).

HESSD
12, 12703–12746, 2015

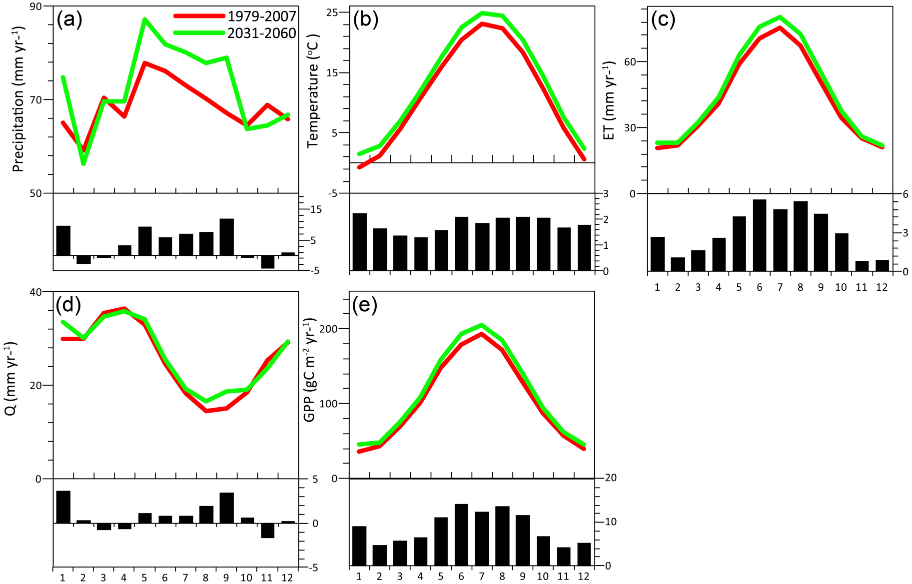

Figure 5. Monthly precipitation **(a)**, temperature **(b)**, ET **(c)**, *Q* **(d)** and GPP **(e)** for the whole CONUS during 1979–2007 and 2031–2060 (the top of each panel), and their differences (future–baseline) between the two periods (the bottom of each panel).

HESSD
12, 12703–12746, 2015

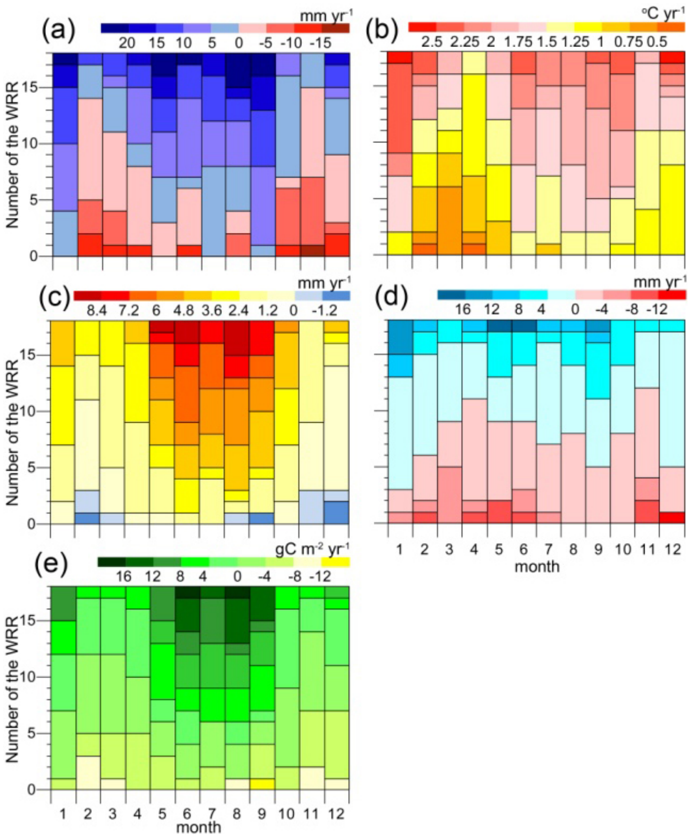

Figure 6. Number of the WRR within a given interval of change (future minus baseline) for each month. **(a–e)** is for precipitation (*P*), temperature (*T*), ET, *Q* and GPP, respectively. The rectangle size for each month represents the number of the WRR that fall in a given interval value.